

## Recent Developments in Solar Photovoltaics and Thermal Hybrid Technology

*Karan C. Prajapati\*, Jatin Patel*

Department of Mechanical Engineering, School of Technology,  
Pandit Deendayal Petroleum University, Gujarat, India

### Abstract

The electrical performance of solar PV panel decreases with increase in the panel/module temperature which is cause of concern in the summer season. To decrease the effect on electrical performance due to increase in module temperature, heat is extracted from the module and used as thermal energy. Heat exchanger or heat extraction device is put on the rear surface of the PV panel and working fluid or coolant is flowed in the heat extraction device. The working fluid used is water, air; refrigerant or combined. This keeps the module surface temperature in limit. Thus the whole configuration of system is known as Solar Photovoltaic/Thermal (PV/T)-Hybrid System. As end-result, we get electricity along with thermal energy which optimizes the system performance. Study conducted on recent development in PV/T hybrid solar collector technology has been discussed in this paper. The effect of collector design and working fluid on the electrical efficiency and thermal efficiency have also been discussed along with the various parameters- solar radiation intensity, rise in temperature of working fluid, etc.

**Keywords:** PV/T Hybrid, solar radiation, electrical efficiency, thermal efficiency, absorber

\*Author for Correspondence Email: karan.pmc11@sot.pdpu.ac.in

### INTRODUCTION

Silicon and germanium are two semi-conductors which are used in making of solar cells. As we already know, the electrical efficiency of solar panel/module ranges from 12% to 16% under standard testing condition (solar spectrum of AM 1.5, irradiance of 1000 W/m<sup>2</sup> and module temperature of 25 °C. For mono and poly silicon solar panels, the electrical efficiency decreases about 0.45%/°C. For amorphous silicon, the electrical efficiency decreases about 0.25%/°C [1]. It is because the temperature of PV module is increased by absorbed radiation which is not converted into electricity resulting in decrease of electrical efficiency. The main problem is in the semi-conductor because increase in temperature decreases the band gap of a semi-conductor the distance between valence band and conduction band decreases. So, there is increase in the flow of electrons as they require lower energy to break the bond as shown in Figure 1.

This results in increase of short circuit current whereas decrease in the open circuit voltage which decreases the maximum power output.

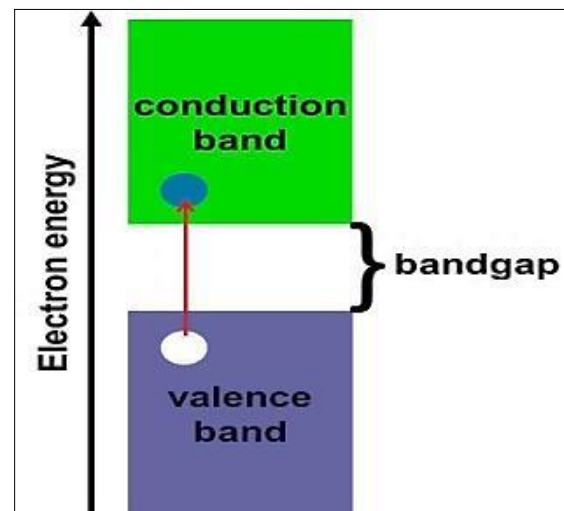


**Fig. 1:** The Distance between Conduction Band and Valence Band.

The blue curve (2) in the graph is at the normal condition whereas the red curve (1) shows temperature rise effect on the maximum power output. It clearly shows the decrease in maximum power output as shown in Figure 2. To decrease this effect of temperature rise on electricity output of solar panel, the concept of solar photovoltaic and thermal is introduced.

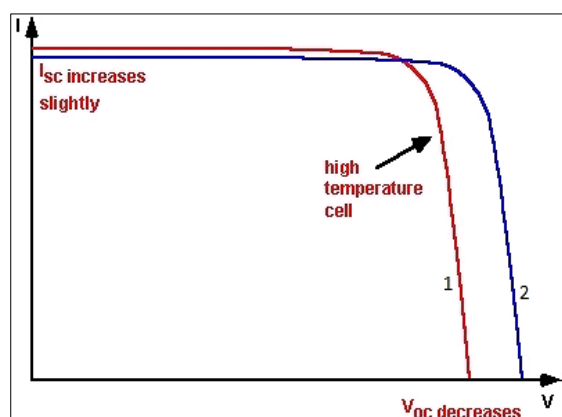


Fig. 2: Effect of Temperature on the IV Characteristics of a Solar Cell [2].

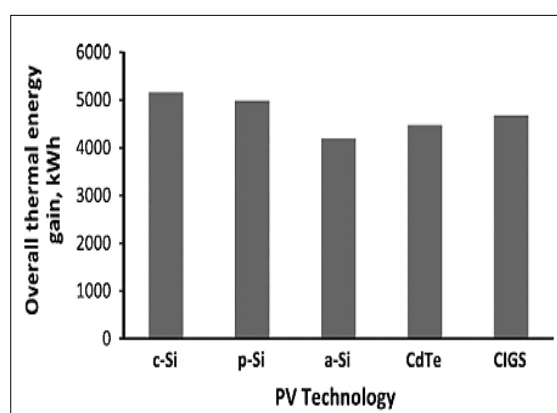


Fig. 3: Annual Overall Thermal Energy Gain with different PV Technology [19].

## SOLAR PHOTOVOLTAIC AND THERMAL-HYBRID SYSTEM

As 15 to 20% of incident radiation is converted into electricity, rest of the incident radiation gets absorbed and converted into heat energy resulting in increase in the temperature of the solar module (in Figure 3). Working fluid flows on or under the surface of solar PV panel to cool the surface of panel, which helps in increasing efficiency of PV panel. The heat is extracted from the surface by cooling using heat extraction device. This extraction device is coupled with solar photovoltaic panel which makes it a hybrid system. On the contrary, it increases working fluid's temperature. But it is necessary to keep working fluid's temperature as low as possible so that more heat can be extracted. At the end, we get electrical and thermal energy. This concept helps in optimizing the electrical efficiency and as byproduct we get thermal energy in Figure 4, achieving a higher energy conversion rate of absorbed solar radiation.

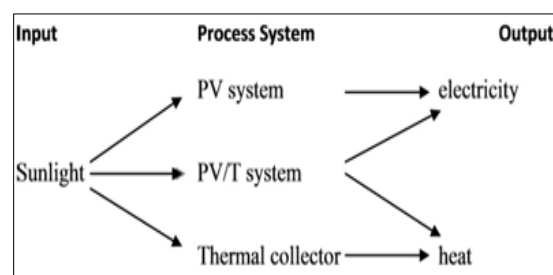


Fig. 4: Benefit of Solar PV/T System.

Solar PV/T systems provide a higher energy output than standard PV modules and could be cost-effective if the additional cost of thermal unit is low. Generally, solar PV/T systems are classified based on the working fluid – air type and water type while refrigerant are exceptional type and glazed or un-glazed. The whole system is covered in an insulated collector with a glass cover over head of PV panel because of which the system achieves higher thermal efficiency than standard PV/T system but gets lower electrical efficiency and is called glazed type solar PV/T system whereas unglazed type solar PV/T system is regular system with no glass cover. They show good electrical efficiency than glazed solar PV/T system but lower thermal efficiency than glazed solar PV/T system, as shown in Figure 5. In building integrated photovoltaic/thermal system, the photovoltaic panels are fixed on the walls of the buildings where the sunlight is more than in other parts of the building. They are fixed at some distance from the wall. The working fluid, normally air or water, is passed between the wall and PV panel. This helps reduce the heat load through the wall. These are the simple types of the solar PV/T systems based on which many designs are made of the systems and tried out. The other classification can be done based on the various designs of the system as shown in Figures 7 and 8.

Sheet-and-tube is a conventional design which is used for solar collectors as shown in Figure 6. The thermal efficiency of a sheet-and-tube collector depends on its ratio of  $W/D$ , in which  $W$  is the distance between the tubes and  $D$  is the tube diameter. The  $W/D$  ratio used in practice is conciliation between optimized heat transfer and economic aspects. However, the optimum for a PV/T system is different for a conventional solar thermal collector. In addition, there are two effects in reduction of the

W/D ratio; one is the increase of the fin efficiency due to the shorter fin length, while the other is a decrease of the flow velocity in the case of parallel risers (due to the increased flow area, assuming the flow rate is kept constant) or an increase in pressure drop in the case of a spiral tube [4]. The thermal efficiency was approximately halved when the tube

spacing to tube diameter ratio (W/D) was increased from 1 to 10 (by keeping W constant) [5]. Efforts have been made to improve the heat transfer from the absorber to the liquid. The best heat transfer is obtained by leading the heat-collecting medium through a thin channel over the full width of the absorber.

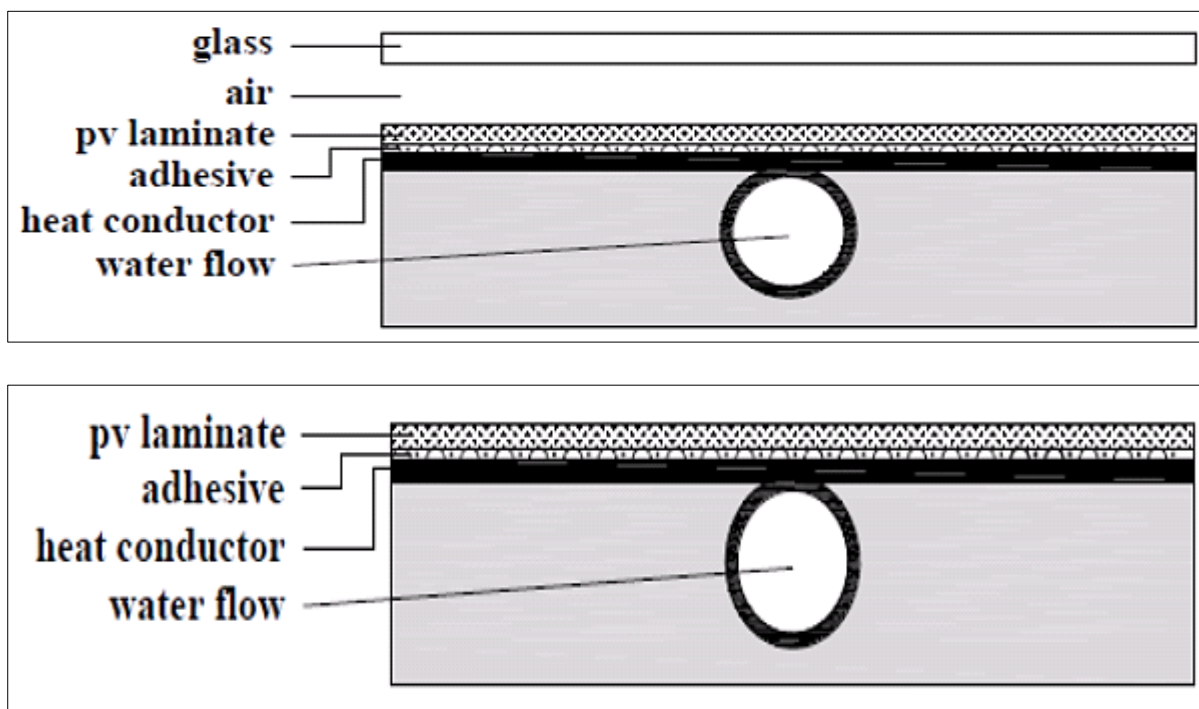


Fig. 5: Glazed and Unglazed Type System [1].

### Various Designs of Solar PV/T System

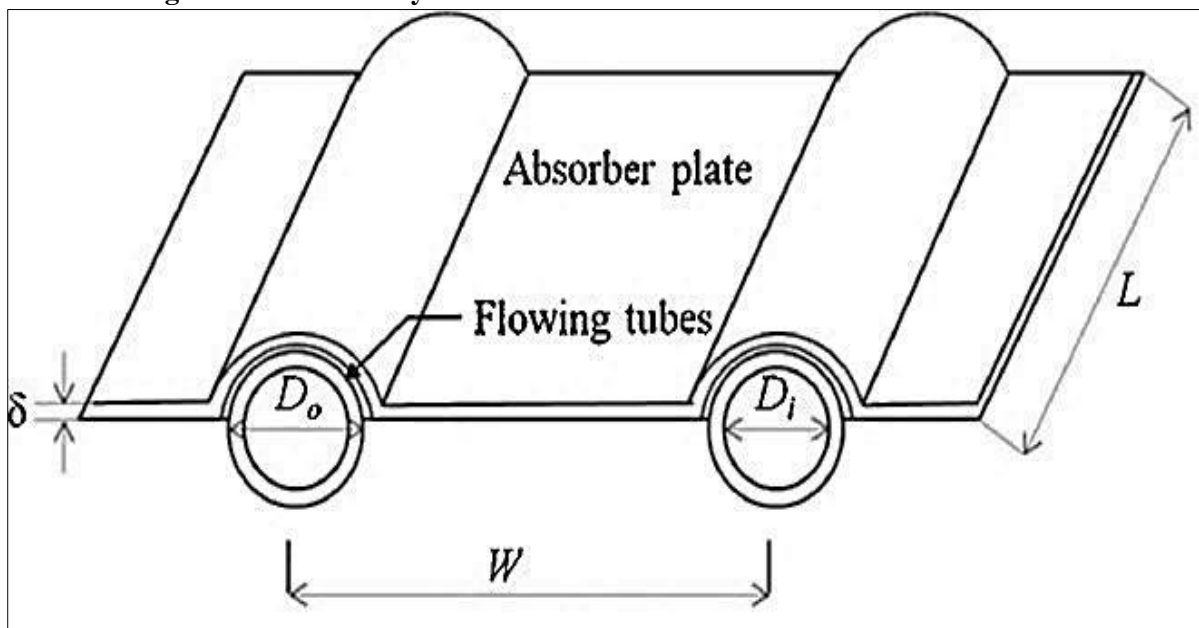


Fig. 6: Sheet-and-Tube Thermal Collector [3].

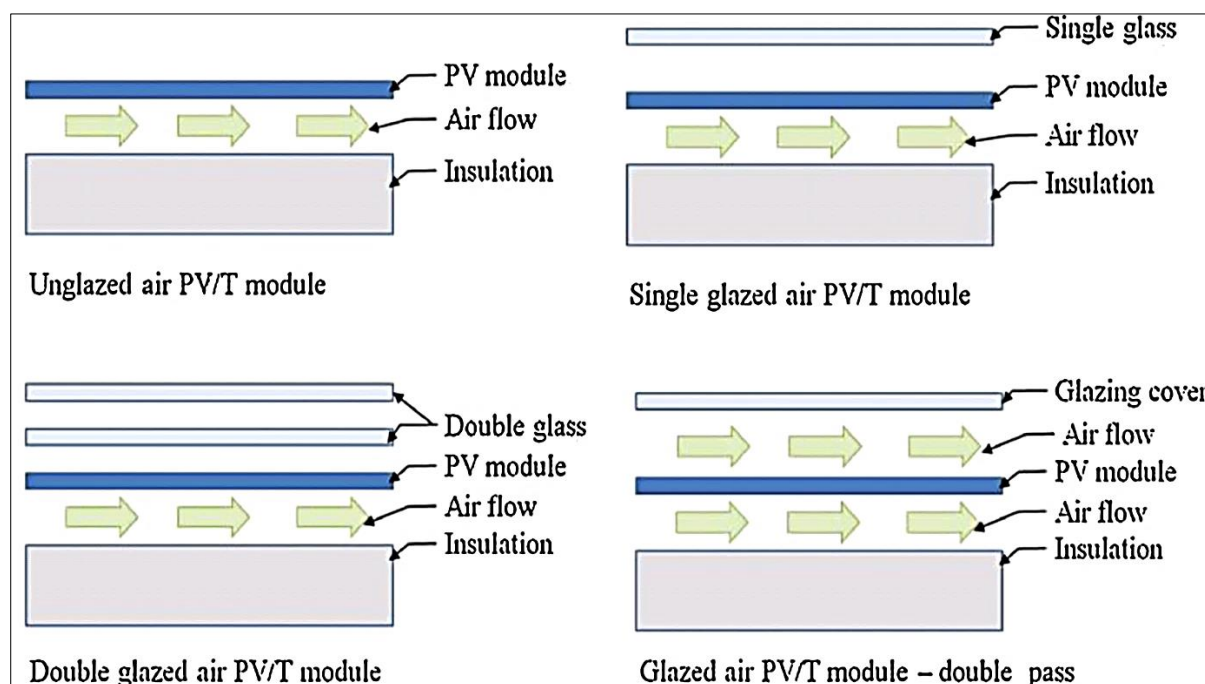


Fig. 7: Cross-Section of Air Type Solar PV/T System [3].

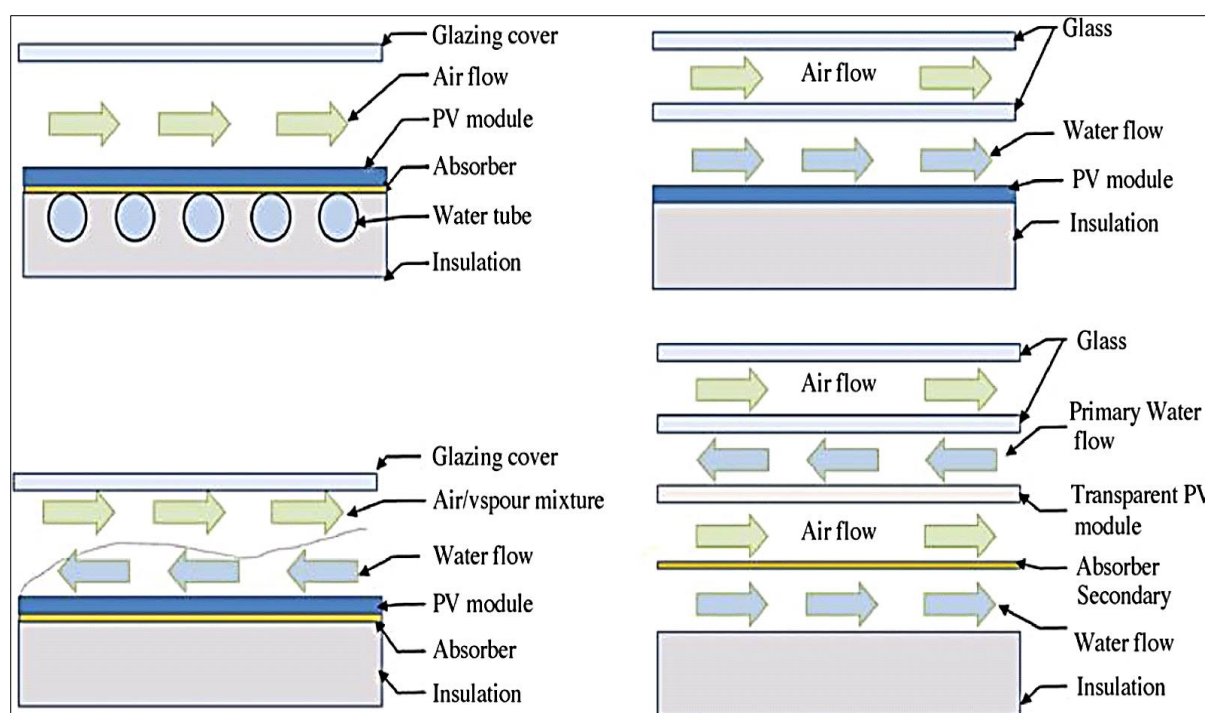


Fig. 8: Cross-Section of Water Type Solar PV/T System [3].

For practical purposes the collector efficiency factor ( $F_0$ ) and the heat removal factor ( $F_R$ ) of a PV/T collector could be considered identical to the ones corresponding to a thermal collector. The thermal performance of a coverless PV/T collector is reduced especially at high temperatures due to heat losses from the top. However, the coverless PV/T collectors have a better electrical performance [5].

### METHODOLOGY

#### Air-Type Solar PV/T Collector

They are simple low-cost system. Air is naturally or forced circulated into the system. They are used for space heating in winter. This system is less effective if the ambient temperature is over 20 °C. They are generally used with fully wetted absorbers. They are less effective than water-type solar PV/T system.





*Fig. 9: Photograph of Wooden Duct with Air Flow Configuration [6].*

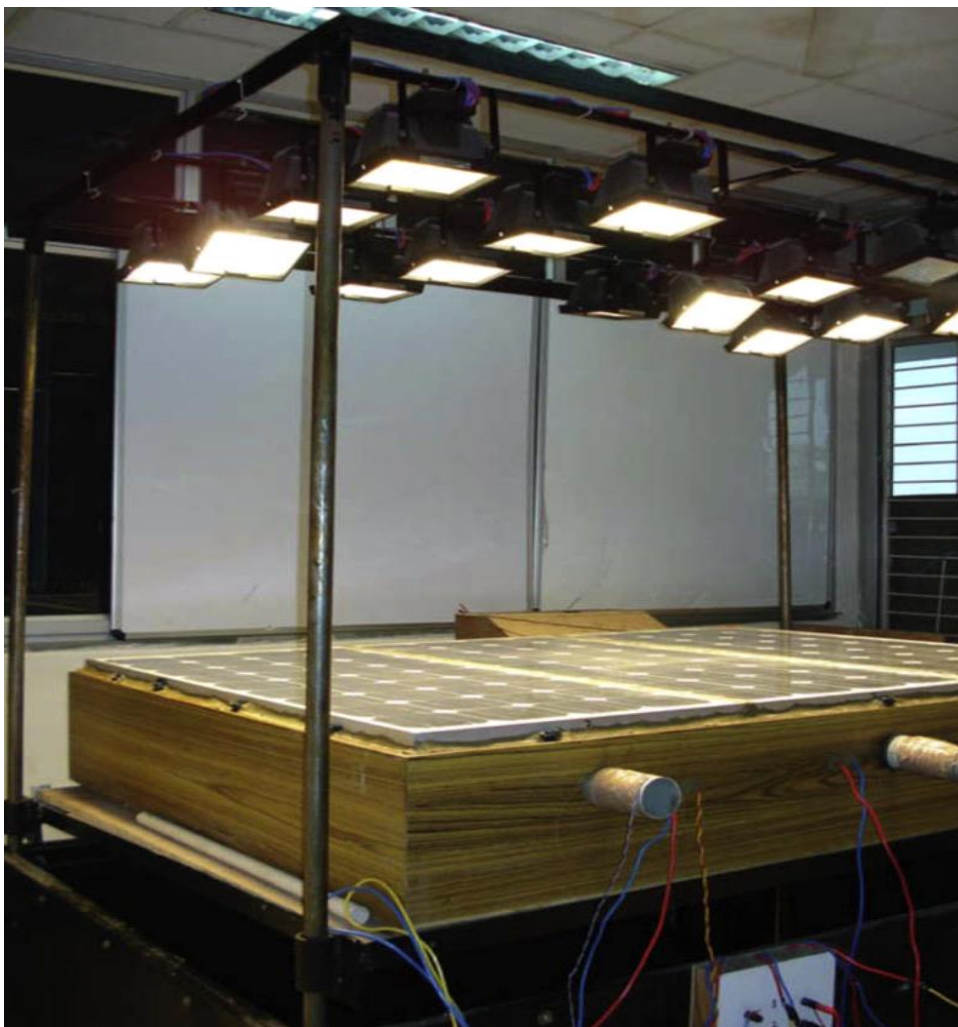


*Fig. 10: Solar PV/T Air Heater with Solar Stimulator [6].*

Dubey *et al.* [6] did an indoor standard test procedure for thermal and electrical testing of PV/T collector connected in series to conduct experimental and theoretical experiment. They developed an experimental stimulator consisting of three PV modules (mono-crystalline silicon solar cells) of glass to tedlar type, each rated at 75 Wp having 1.2 m length and 0.45 m width mounted on a wooden duct. There is a provision for inlet and outlet air to pass below the PV module through the duct. Air duct is sealed with putty and adhesive tape to avoid air leakage. There is also a provision for varying the depth of duct by using number of thermocol sheets. Similarly, another two

collectors are fabricated and connected in series through PVC pipe. Collectors are arranged in such a manner that outlet of first collector is inlet of second collector and outlet of second collector is inlet for the third collector (Figures 9 and 10). A mild-steel platform is fabricated with a mechanism for up and down movement. A DC fan of 12 V and 1.5 A is used for circulation of air and a rheostat is used for varying the mass flow rate of flowing air. PV/T air collectors are tested under solar simulator which has 16 tungsten halogen lamps each having 500 W and rated at 240 V and 11 A. The halogen lamps are arranged in  $4 \times 4$  metrics for uniform distribution of irradiance.

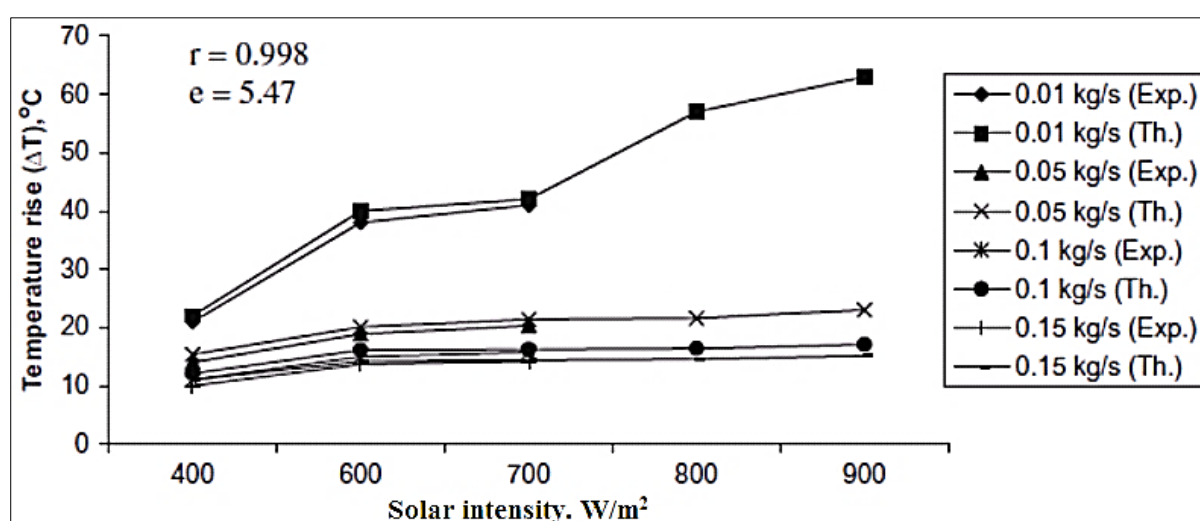


Fig. 11: Effect of Air Temperature Rise by Varying Mass Flow Rate and Radiation Intensity at Inlet Air Temperature 38 °C [6].

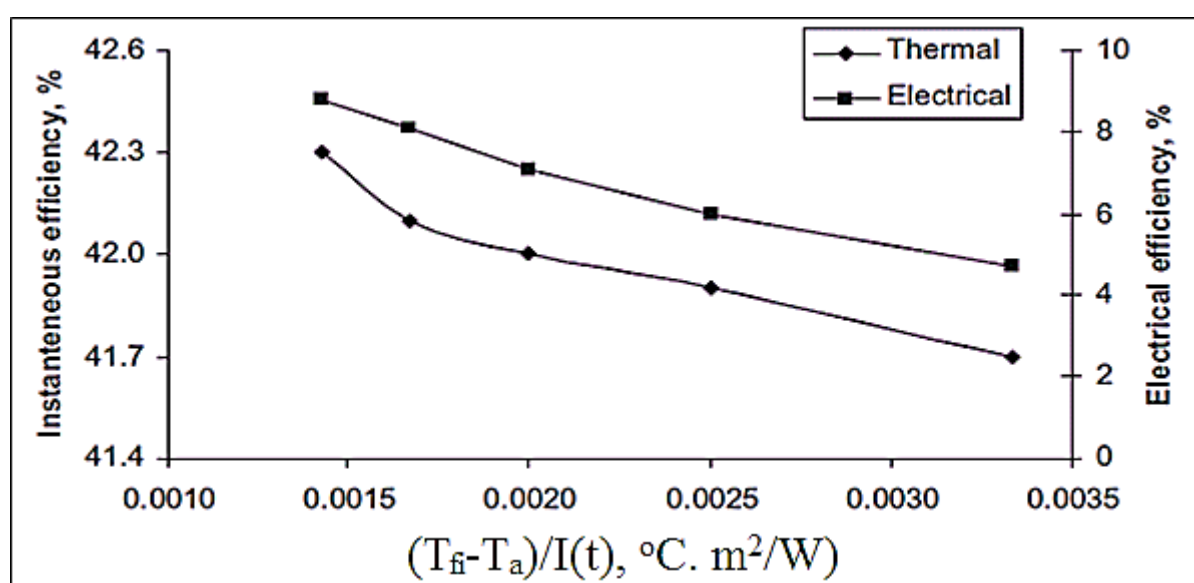


Fig. 12: Variation of Instantaneous Efficiency and Electrical Efficiency with Zero Reduced Temperature [6].

The authors varied the mass flow rate of air and solar radiation intensity to see the effect on the outlet air temperature rise and electrical and thermal efficiency. The inlet air temperature is kept fixed for every reading. The rise in temperature decreases with increase in mass flow rate and solar radiation intensity reaching towards steady state condition. Experimental and theoretical results are validated for 400, 600 and 700 W/m<sup>2</sup>, in Figure 9. The thermal, electrical and overall efficiency of the solar air heater are 42, 8.4 and 50.0%, respectively as shown in Figure 12. Othman *et al.* [7] documented various research activities done in Solar Energy Research Institute, National University of Malaysia, about solar PV/T collector system using working fluid as air. They concluded that out of various designs, double-pass solar PV/T collector with fins and CPC showed better electrical and thermal performance than other models in Figure 13.

Increasing the flow rate will increase the heat transfer coefficient between the channel walls and the working fluid, resulting in a lower mean photovoltaic cell temperature.

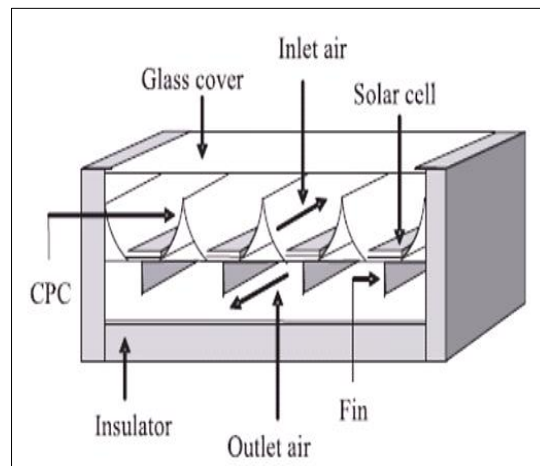


Fig. 13: Schematic Diagram of Double-Pass PV/T Collectors with Fins and CPC [7].

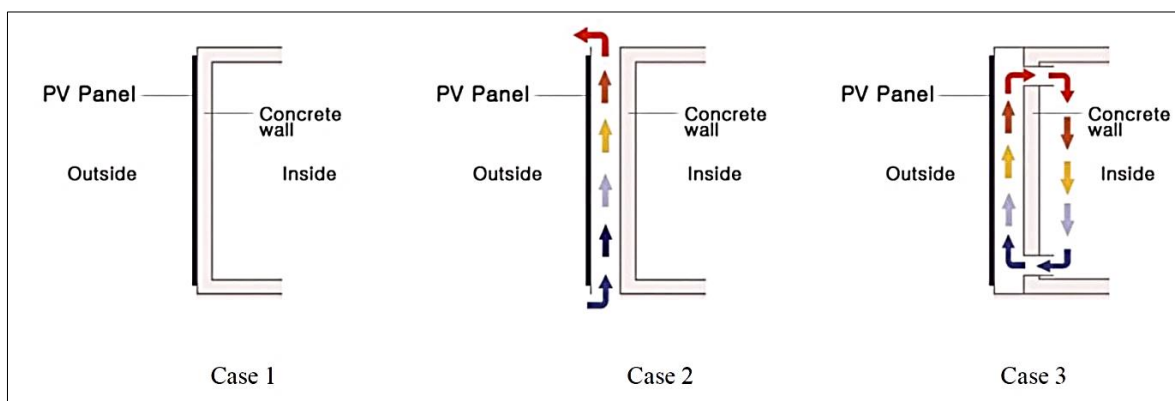


Fig. 14: Building Façade Design with BIPV and BIPVT Systems for Simulation Mode [8].

Table 1: Simulation Model for Building with BIPV and BIPVT System [8].

Name	Model Description
Reference Case	Building in which BIPV system is not installed
Case 1	Building in which BIPV system was attached to building envelope (without an air layer between PV panels and walls)
Case 2	Building in which force ventilated BIPV system was applied as building envelope (with 10 cm air layer between PV panels and wall, outdoor air inflow to air layer at a rate of 0.02 kg/s m <sup>2</sup> )
Case 3	Building in which BIPV-Thermal system was applied as building envelope (with 10 cm air layer between PV panels and wall, indoor air inflow to air layer at a rate of 0.02 kg/s m <sup>2</sup> )

This will increase the electrical efficiencies of the collector. The combined efficiency varies from 39 to 70% at mass flow rate of 0.015–0.16 kg/s and radiation intensity at 500 W/m<sup>2</sup>. Kim and Kim [8] developed a simulation model of an air-type BIPV/T system integrated

into the building facade and the annual energy performance of the building with the air-type BIPV/T system installed on its envelope was analyzed through simulation modeling using the TRNSYS simulation program with the sub-models of Type 567 and Type 56 as

shown in Figure 14. For the simulation, a two-story office building was modeled with three zones. The first floor has one zone (590 m<sup>2</sup>) and second floor has two zones (498 and 60 m<sup>2</sup>). It was assumed that the office building is located in Daejeon, Republic of Korea (latitude 36.32N, longitude 127.38E). The hourly weather data of Daejeon as TMY form was used. The zone temperature is controlled to 20 and 26 °C for the heating and cooling. It was also assumed that BIPV or BIPV/T system were placed on the south facade of the building model with 128 PV modules of a total rated power of 16 kWp over an area of 129 m<sup>2</sup>. The air gap distance between BIPV modules and building wall surface was assumed to be 10 cm and the air flow rate of 9310 kg/h. For the Case 3, it is controlled that the hot air from BIPV/T system is exhausted to outside during the cooling season. It was analyzed that the electricity generation of Case 2 and 3 is higher annual 6 and 3% respectively due to PV module cooling of the BIPV/T envelope than that of building with the BIPV envelope of the Case 1. These results indicate that BIPV/T system certainly improves the electricity generation during the winter season, because the forced air flow significantly cools the PV modules. On the other hand, the BIPV/T system that circulates the indoor air showed a

lower increase in electricity generation compared to the BIPV/T system with outdoor air inflow. Therefore, the BIPV/T system with outdoor air inflow is more advantageous from a PV module cooling aspect; however, the BIPV/T system that circulates the indoor air and runs the obtained heat source indoors is favorable in terms of building heating and cooling, along with overall energy, because the effect of the heating energy reduction is relatively greater than that of the electricity generation increase. The thermal efficiency of Case 2 and 3 are average 30 and 14% respectively in the winter season that solar radiation is higher than that of the summer. The BIPV/T system was found to be more useful due to its increased electrical efficiency and heating energy conservation in winter in comparison with the BIPV system (Figure 15), which does not take into consideration the rear ventilation. Air has a thermal conductivity that is 24 times lower than for water. Since  $h = N_u \cdot (k/D)$ , this reduces the heat transfer. This leads to the fact that for air collectors the channel height has a large influence on the thermal efficiency. Due to the much lower heat capacity the flow rate in an air collector is necessarily much larger than in a liquid collector [4]. Solar PV/T systems are helpful for CO<sub>2</sub> mitigation and earning the carbon credits [9].

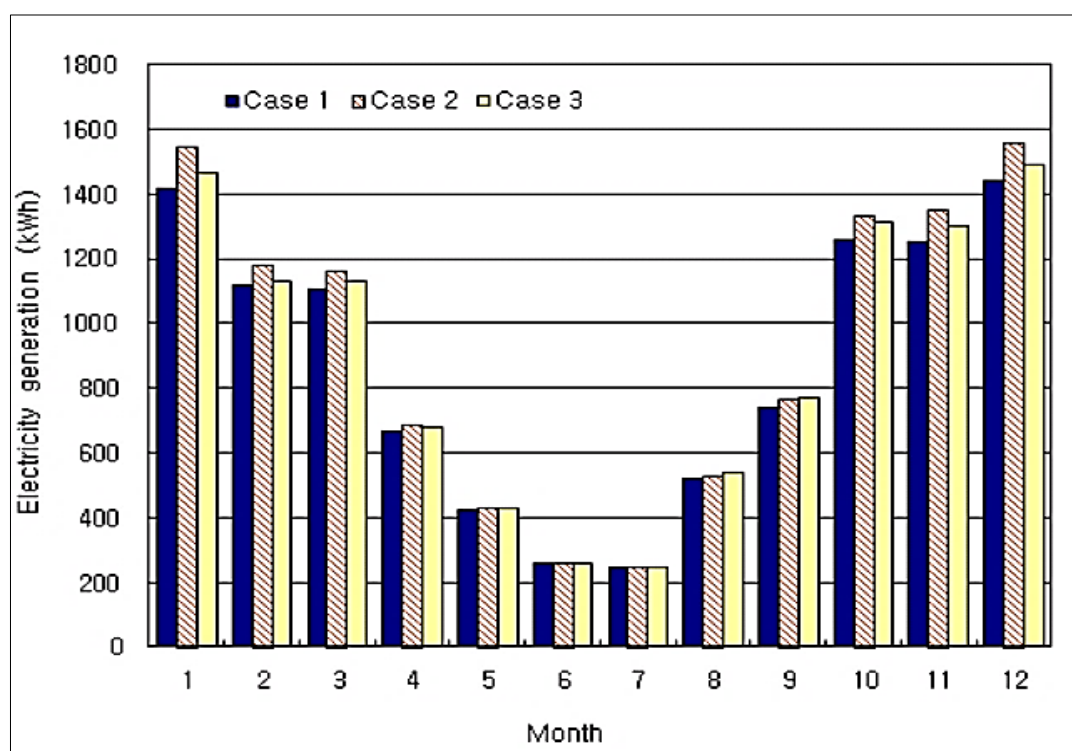


Fig. 15: Monthly Electricity Generation of Three Cases [8].



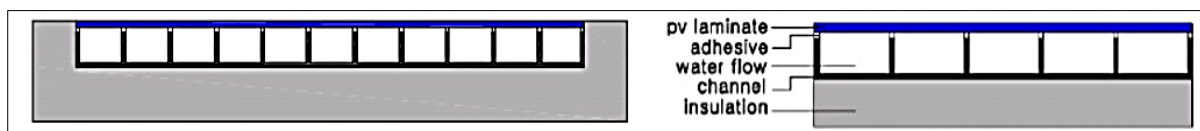


Fig. 16: Sectional View of the Unglazed Solar PV/T Collector with Fully Wetted Absorber [10].

### Water-Type Solar PV/T System

Forced circulation of water is done in the system to increase the heat transfer rate. They are more effective but more expensive than air-type system. They are used for domestic hot

water usage for daily purpose. Their efficiency is more than that of air-type system. They are generally used with fully wetted (Figure 16) or sheet-and-tube absorbers.



Fig. 17: Experimental View of the PV/T System and the PV Module; Measuring Equipment [10].

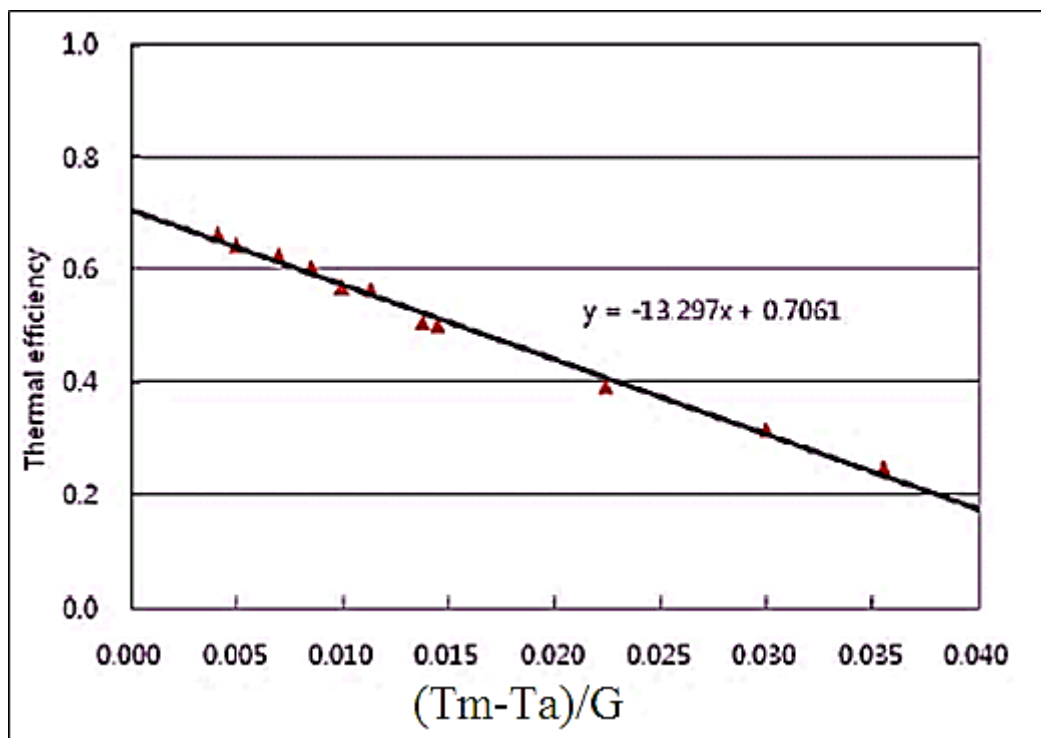


Fig. 18: Thermal Efficiency of the Unglazed PVT Collector with a Fully Wetted Absorber [10].

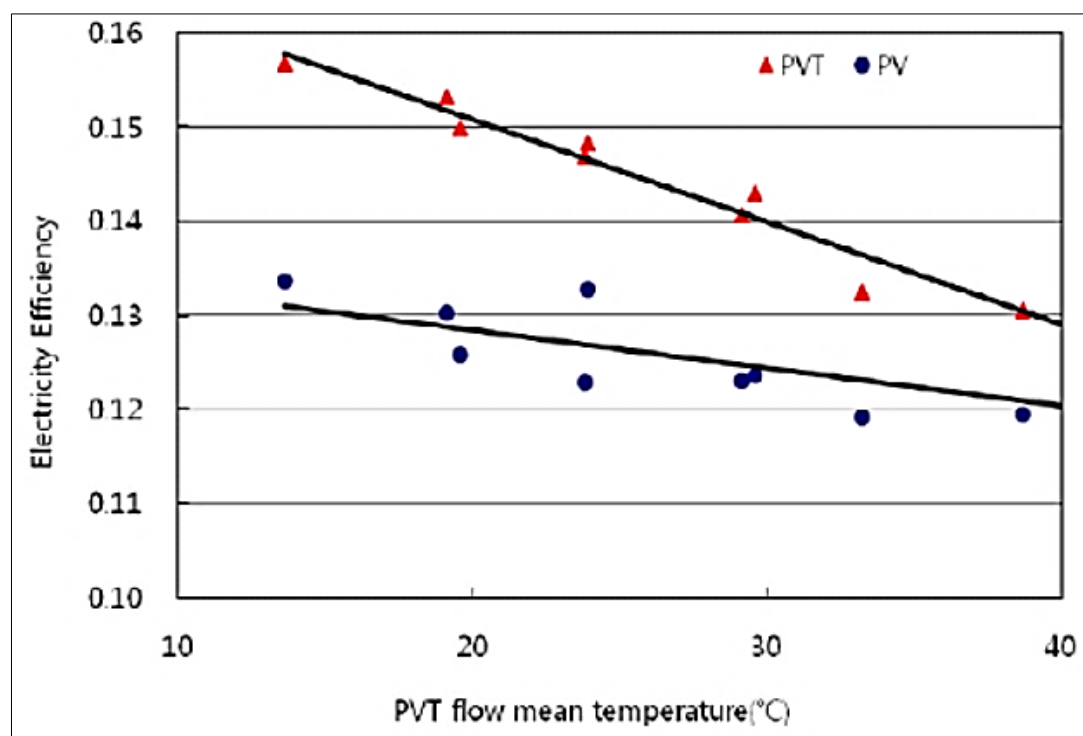


Fig. 19: Electrical Efficiency of the Fully Wetted PVT Collector and a PV Module [10].

Kim and Kim [10] did an experiment to analyze the electrical and thermal performance of a water-type solar PV/T collector with fully wetted absorber and unglazed in outdoor conditions as shown in Figure 17. A conventional monocrystalline Si PV module was tested alongside the PV/T collector in order to compare their electrical performance. The PV/T collector consists of a PV module and fully wetted heat exchange units made of aluminum plates. The aluminum channel, a fully wetted absorber, was attached on the backside of the PV module with thermal conduction adhesives. The PV/T collector had no additional glass cover, and was thermally protected with 50 mm of thermal insulation. The PV module used for the PV/T collector was a 240 Wp mono-crystalline silicon PV module; its electrical efficiency was 16.5% at STC. The PV/T collector with fully wetted absorber was tested at a solar radiation level that exceeded  $790 \text{ W/m}^2$  and at a water flow rate of  $0.02 \text{ kg/sm}^2$ . The electrical and thermal performance measurements were carried out under a quasi-stationary condition in an outdoor environment at the same time. The fully wetted PV/T collector had the overall energy performance of about 65%, combining the average values of its thermal and electrical efficiencies. The average electrical efficiencies of

the PVT collector and the PV module are 14.3 and 12.6%, respectively, and their difference reaches a maximum of 2.4% and has an average of 1.7%. The electrical efficiency of the PV/T collector depends on the fluid temperature, which can directly affect the PV module temperature (Figure 19); the electrical power is high under the condition of lower fluid temperature. The average thermal efficiency of the PV/T collector is about 51% under outdoor test conditions (Figure 18). It is also obvious that the thermal performance of the PV/T collector is relatively poor compared to the other collectors, since the front plate of the PV/T collector consisting of PV module with solar absorber lose more heat and solar radiation reaches indirectly on the absorber.

Jaiganesh and Duraiswamy [11] did an experiment on glass to tedlar (G2T) PV panel and glass to glass photovoltaic thermal system (G2G-PVTS) to analyze the thermal performance and electrical performance as shown in Figures 20 and 21. They took two system-G2G PV panel integrated with thermal system and G2T type PV panel. The solar collector area size of G2G PV panel was  $775 \times 650 \text{ mm}$  and the thickness of the panel was 7 mm. This G2G PV panel was placed over the frame of the thermal system in the size of length, breath

and height of  $805 \times 680 \times 95$  mm respectively. The cooling system inside the frame with six

numbers of copper fins in the size of 640 mm length and 118 mm breadth was placed.

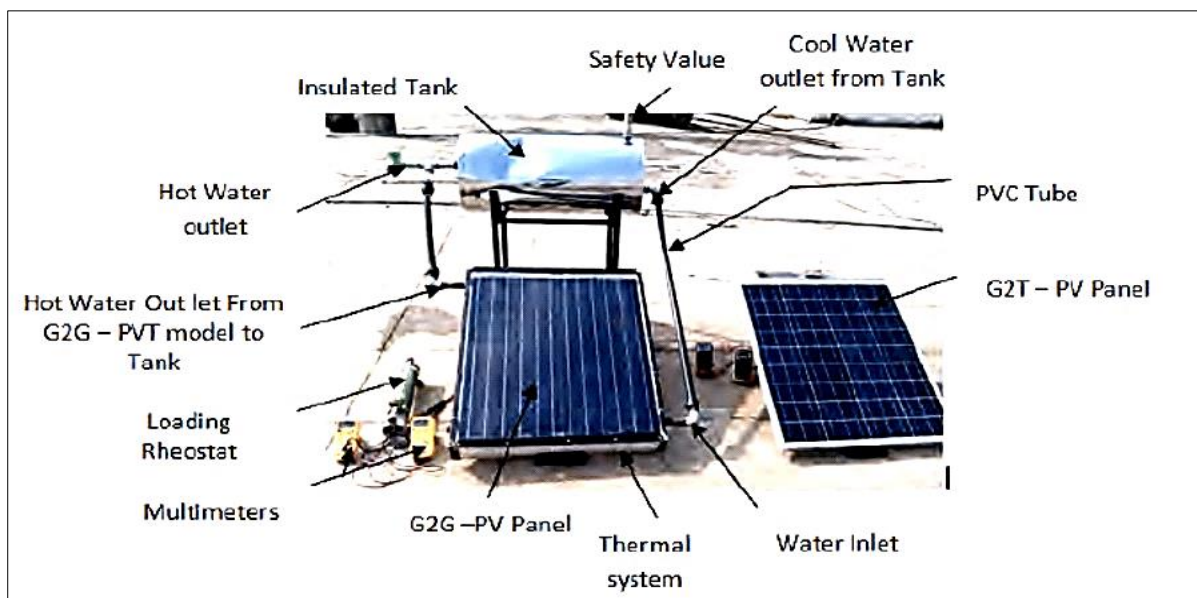


**Fig. 20:** Experimental Setup of G2G PV Panel Combined with Thermal System and G2T PV Panel [11].

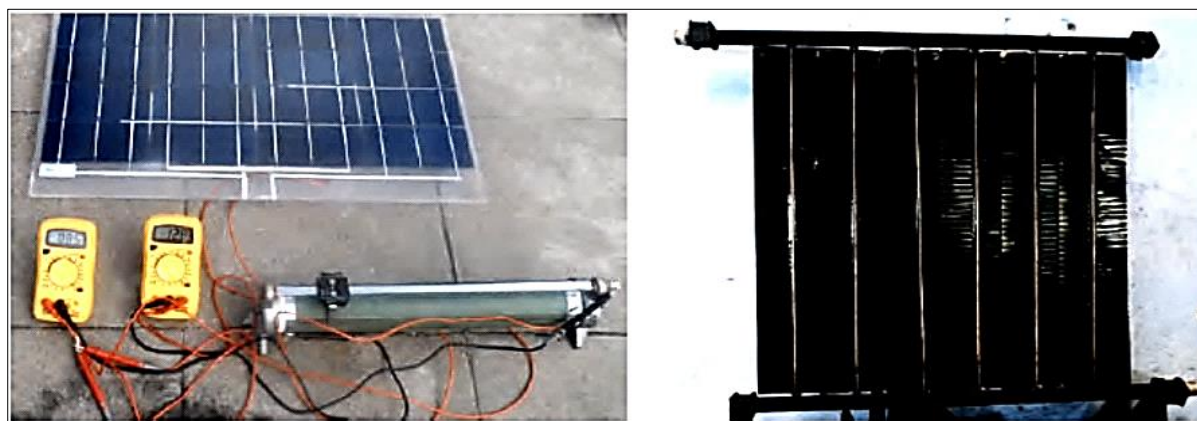


**Fig. 21:** (Left) Glass to Glass PV Panel and (Right) Copper Fins Arrangement between Header Tubes [11].

The average efficiency of G2G PVT and G2T PV Panels are 11.65 and 10.95% respectively (Figure 22 and 23). The efficiency of G2G PVT was 0.7% higher than G2T PV panel, in addition that the thermal efficiency of the G2G PVT system was 44.37%. The initial temperature of hot water received from the thermal system of G2G PV/T System starts from  $35^\circ\text{C}$  and it reaches maximum up to  $56.8^\circ\text{C}$ . So the overall efficiency of the G2G PV/T system was the addition of both electrical (11.65%) and thermal efficiency (44.37%) is 56.02% for the instantaneous test reading for the particular

time. The result showed that when the solar radiation increased, the electrical output also increased along with temperature. The range of temperature increased between  $44.9$  to  $72.5^\circ\text{C}$  on the PV cell in G2G-PV panel, it was above the STC temperature of  $25^\circ\text{C}$ . At this temperature, the G2T panel power generation was slightly higher than G2G-PV. Then the G2G-PVT panel was tested with water cooling system then the efficiency gets increased (11.65–10.95%) 0.7% over the G2T-PV panel.

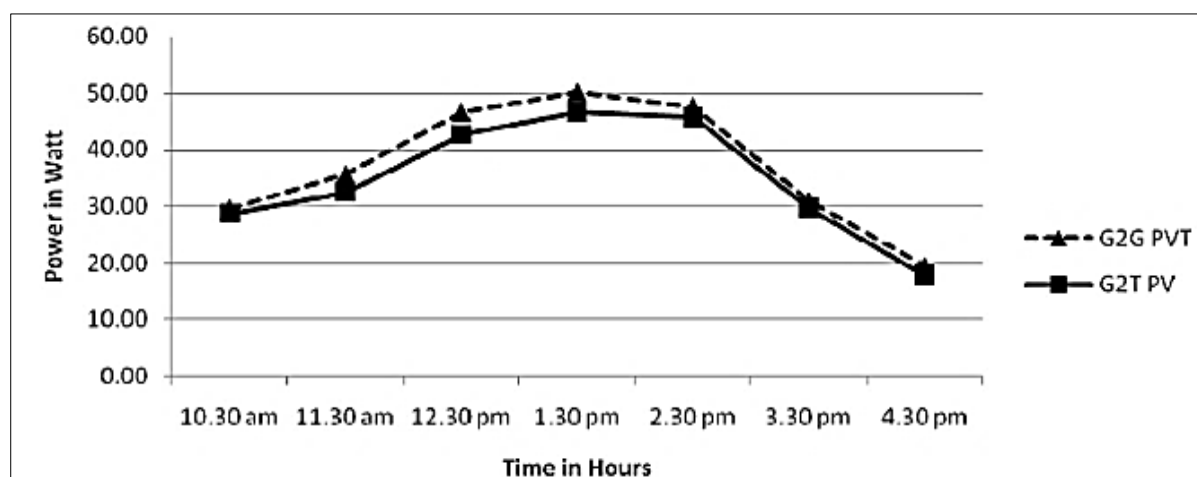


Fig. 22: Maximum Power Output from G2G PV/T System and G2T PV Panel [11].

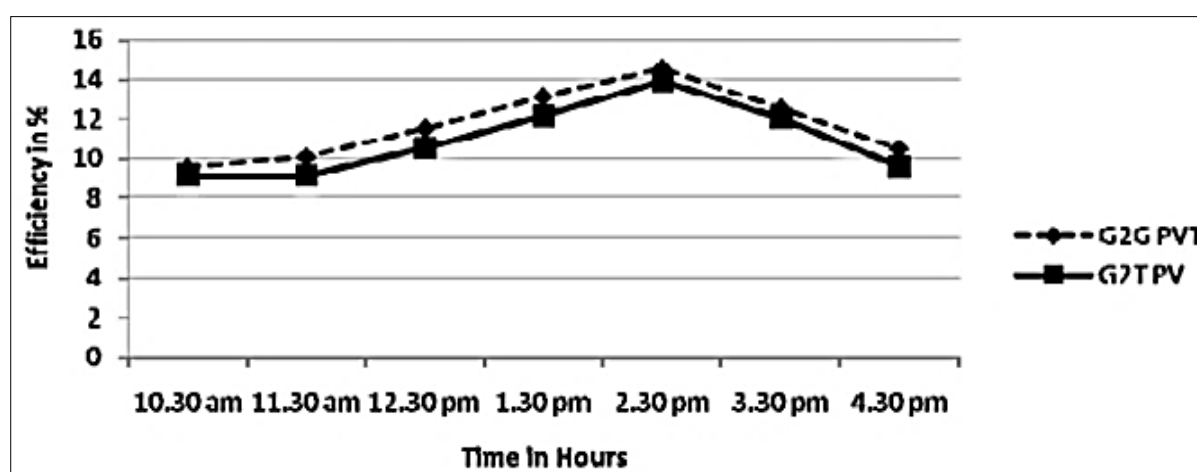


Fig. 23: Electrical Efficiency of G2G PV/T System and G2T PV Panel [11].

Table 2: Values of Coefficients and Ambient Conditions Used in Simulations [12].

Parameter		Value	Parameter		Value
Width of collector	$W_l$	0.53 m	EVA thermal conductivity	$k_{EVA}$	0.35 W/m.K
Length of collector	L	1.183 m	Thickness of Tedlar	$\delta_T$	175 $\mu$ m
Bond width	B	0.01 m	Tedlar thermal conductivity	$k_T$	0.2 W/m.K
Outer diameter tube	$D_o$	0.01 m	Emissivity of PV	$\epsilon_{pv}$	0.88
Inner diameter tube	$D_i$	0.008 m	Emissivity of the back surface	$\epsilon_{bs}$	0.85
Height of air channel	H	0.06 m	Absorptivity of PV	$\alpha_{pv}$	0.9
Width of air channel	$W_a$	0.53 m	Absorptivity of tedlar	$\alpha_T$	0.5
Length of tube segment	$\Delta y_{tube}$	0.42 m	Ambient temperature	$T_a$	302.15 K
Tube spacing	W	0.09 m	Irradiance	G	800 W/m <sup>2</sup>
Thickness of PV cells	$\delta_{pv}$	300 $\mu$ m	Wind speed	$v_w$	2.0 ms
PV cells thermal conductivity	$k_{pv}$	148 W/m.K	Inlet fluids temperature	$T_{fi}$	302.15 K
Thickness of EVA	$\delta_{EVA}$	450 $\mu$ m	The solar cell temperature at reference condition	$T_{ref}$	298.15 K

Chow *et al.* [12] presented annual performance of a building integrated photovoltaic/ water-heating system for a warm climate application

in Hong Kong. The PV/T collectors are integrated on the south wall of an air-conditioned building.



The PV-wall (PV/T water) wall was composed of six PV/T water collectors mounted on a 100-mm brick wall with plastering on both interior and exterior wall surfaces. The PV/T water collector adopted the flat box thermal absorber design and was provided with polycrystalline silicon PV cells. A photograph and constituent layers of the BIPV/T water system are shown in Figure 24. The system thermal performance under natural water circulation was found to be better than the pump-circulation mode. For a specific BIPV/T water system at a vertical wall of a fully air-

conditioned building and with collectors equipped with flat-box-type thermal absorber and polycrystalline silicon cells, the year-round thermal and cell conversion efficiencies were found to be 37.5 and 9.39% respectively under typical Hong Kong weather conditions.

The overall heat transmission through the PV/T water wall is reduced to 38% of the normal building facade. When serving as a water pre-heating system, the economical pay-back period was estimated to be around 14 years.



**Fig. 24:** Experimental Setup of Building Integrated Photovoltaic/Water Heating System at City University of Hong Kong [12].

### Bi-fluid-Type Solar PV/T System

There are two working fluids (normally- water and air) flowing simultaneously in two different heat exchangers/extractors. Sometime one working fluid is stagnant or other at a time. This is done to increase the heat extraction rate from solar PV panel. Abu Baker *et al.* [13] designed a simple unglazed bi-fluid solar PV/T system (Figure 25) which integrates a

conventional serpentine-shaped copper tube flat-plate water solar collector a single-pass air collector. When the water flow is to be kept at 0.0005, 0.0079 and 0.0247 kg/s, the predicted thermal, electrical, and total equivalent thermal efficiencies are 32.6, 10.7 and 62.4; 42.5, 11.0 and 75.0; 46.6, 11.1 and 78.8%, respectively. The simulations were done using Matlab software with 2D steady-state analysis.

PV/T systems with the dual heat extraction operation can be effectively used in houses, residential and office buildings, in hotels, hospitals and also in the industrial and agricultural sectors providing electricity and heat with

flexibility in the heat removal fluid. They are cost-effective solar energy devices, mainly for operation in low temperatures and are promising systems for a wider application of photovoltaics [14–16].

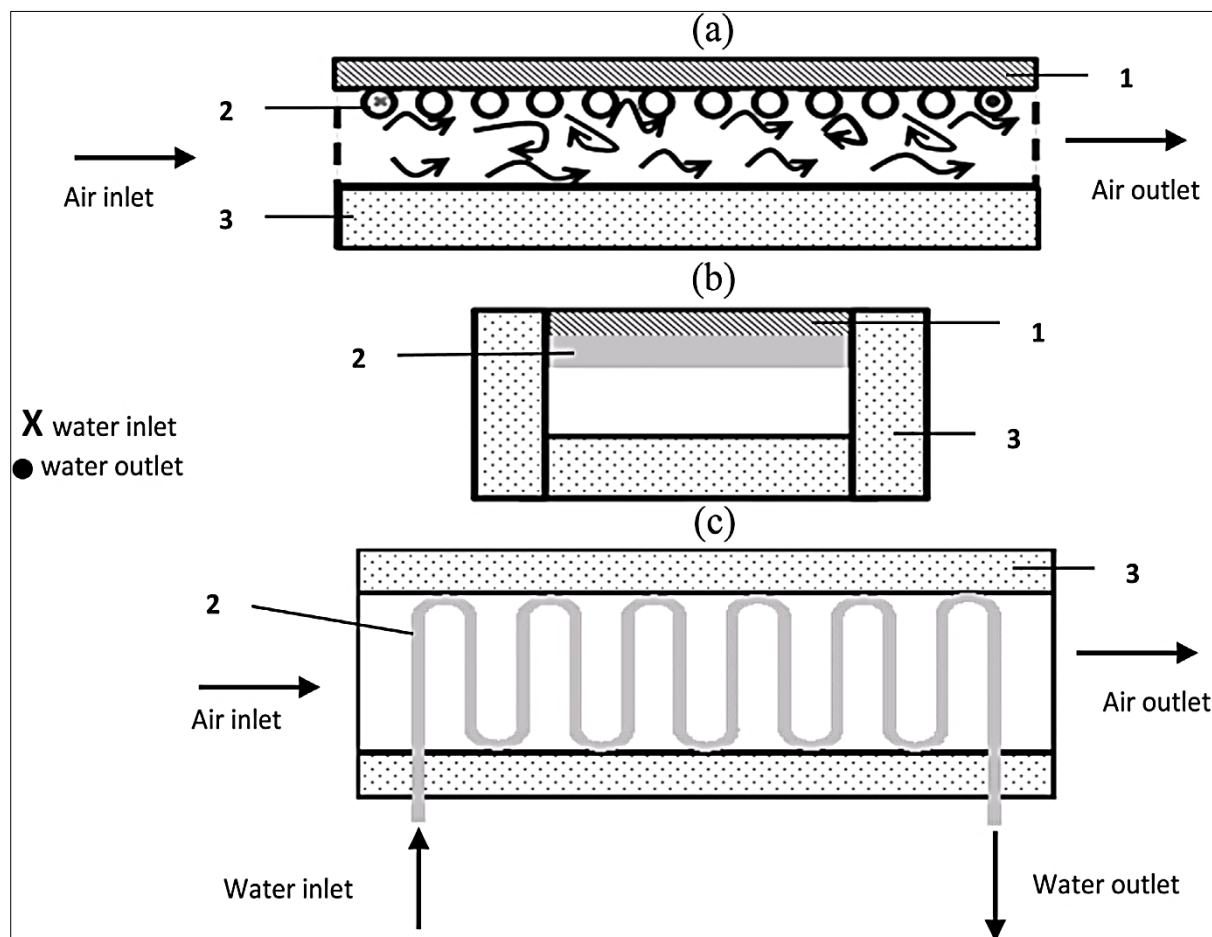


**Fig. 25:** The Schematic Diagram of the Single Pass Bi-fluid PV/T Solar Collector. (a) Side View Cross-Section, (b) Front View Cross-Section, and (c) Top View Cross-Section. The Collector Consists of (1) PV Module, (2) Serpentine Copper Tube, and (3) Insulation Layer [13].

### Refrigerant-Type Solar PV/T system

Refrigerants are used as working fluid to increase the heat extraction rate because they have high specific heat capacity and can be recirculated again and again. This increases the cooling rate of solar PV panel.

Fang *et al.* [14] did modeling solar PV/T system using refrigerant as working fluid under saturated condition in Figures 26 and 27. The main benefit of using refrigerant as working fluid is that the boiling heat transfer coefficient and the condensation heat transfer coefficient of the refrigerants are significantly higher (20 to 100 times higher) than the single-phase convective heat transfer coefficient (air or wa-

ter). A new type of environment-friendly refrigerant, R410a does not destroy the ozone-sphere. It has the advantages of high refrigerating efficiency, excellent chemical and thermal stability. R410a is the world-recognized ideal substitution of the refrigerant R22 so far. Therefore, the refrigerant R410a is employed as the working fluid in this paper.

With the increase of the solar radiation intensity under the constant evaporating temperature, the temperature of the solar cell and the temperature of the backplane rise, the photovoltaic efficiency reduces, and the overall photovoltaic power of the hybrid PV/T collector increases. With the increase of the evaporating tem-

perature under the constant solar radiation intensity, the temperature of the solar cell and the temperature of the backplane rise, while the photovoltaic efficiency decreases, and the overall photovoltaic power of the hybrid PV/T collector decreases. Compared with the PV/T water/air heating collector, the hybrid PV/T

collector using refrigerant as working fluid performs quite well in the photovoltaic performance. From the analysis above, it can be known that the working temperature of the solar cell drops down to a certain degree and the PV module works in an ideal state.

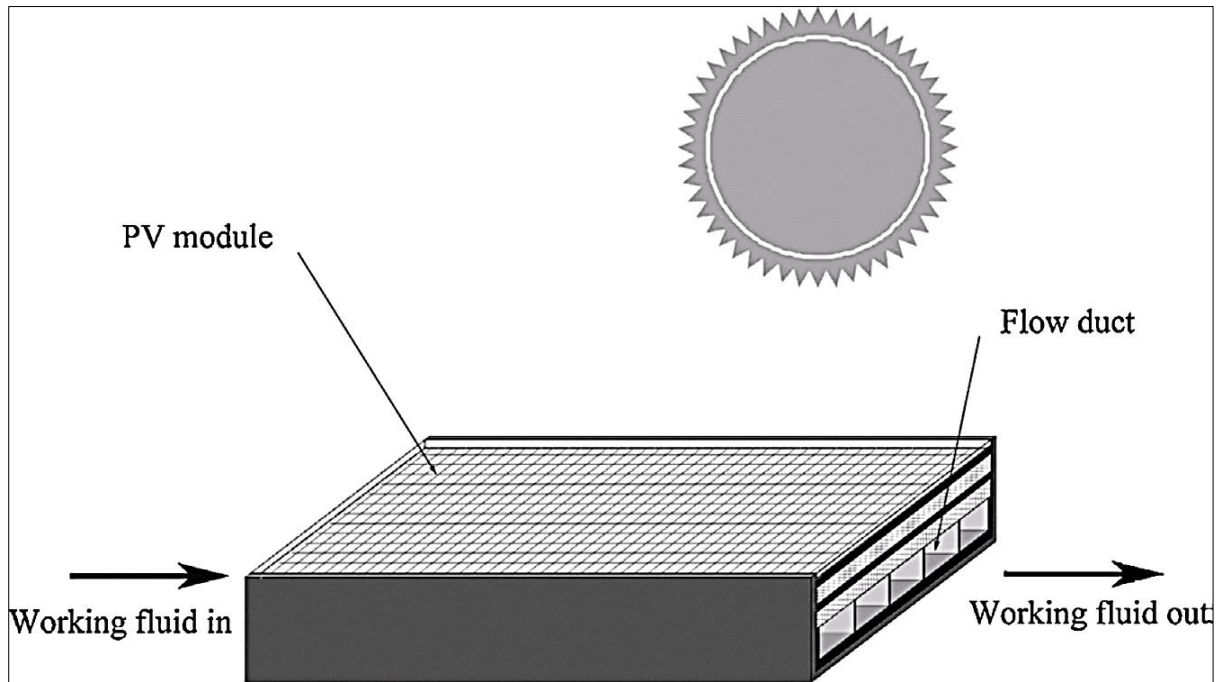


Fig. 26: The Typical Structure of Hybrid PV/T Collector or System [14].

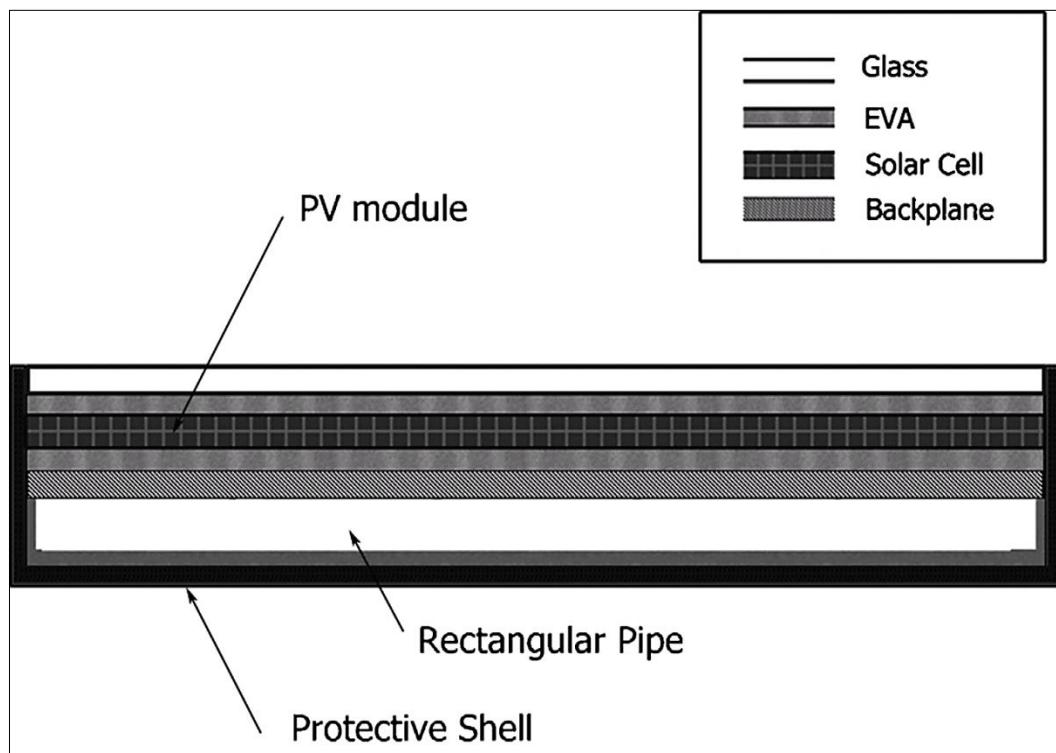


Fig. 27: The Section View of the PV/T System [14].

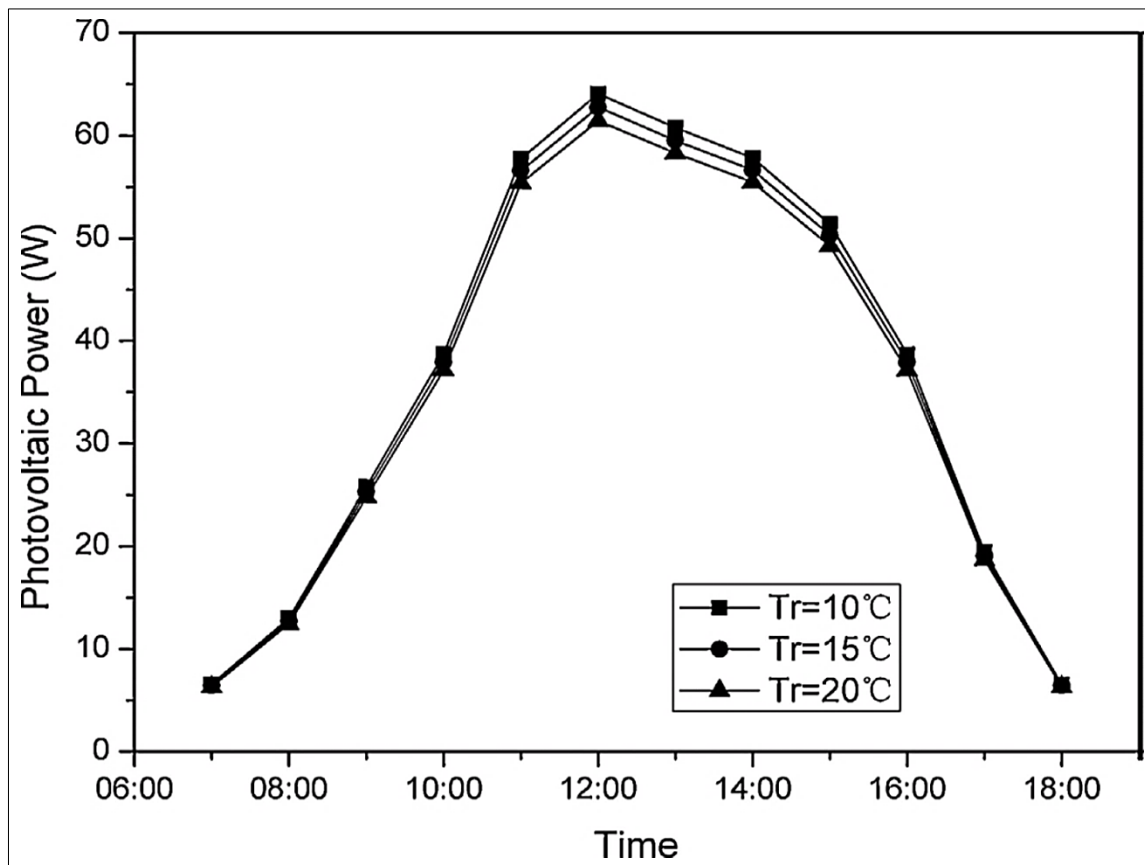


Fig. 28: The Variation of Photovoltaic Power with Time [14].

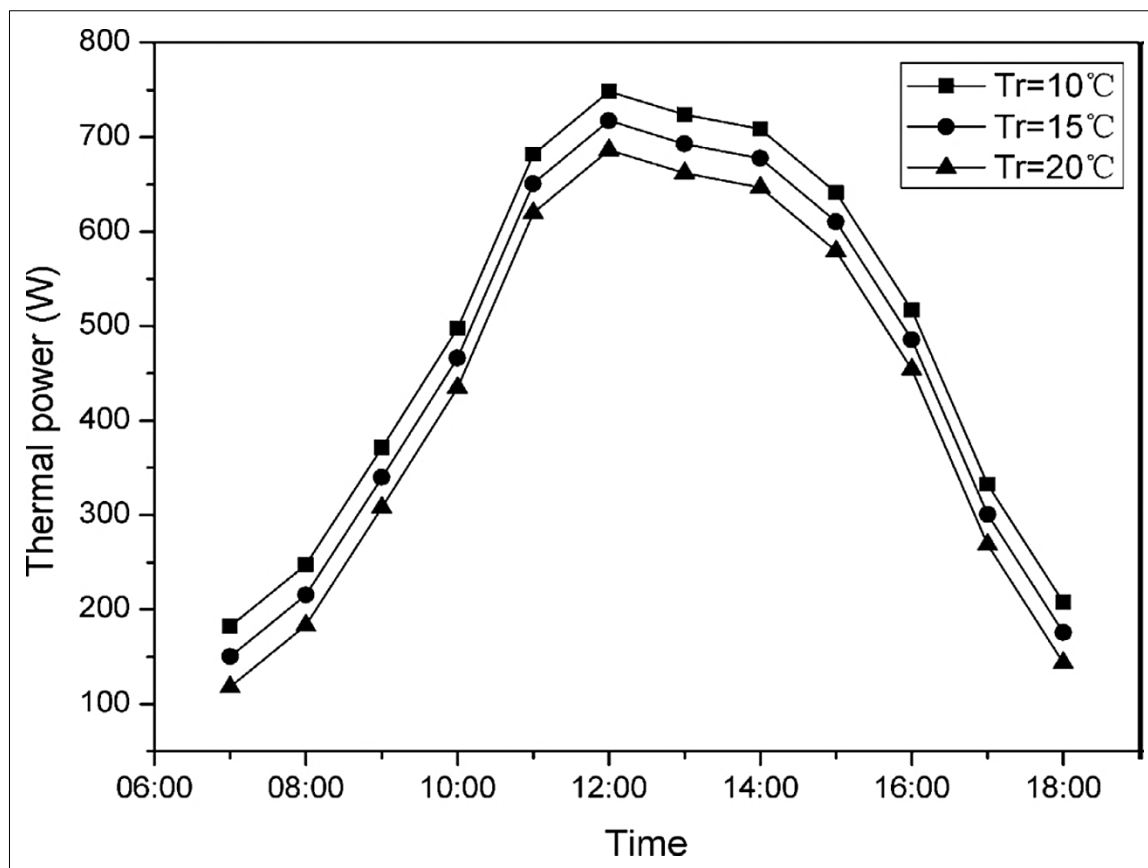


Fig. 29: The Variation of Thermal Power with Time [14].



Refrigerant-based PV/T could significantly improve the solar utilization rate over the air- and water- based systems and therefore has potential to replace the former two systems in the near future. Its performance is largely dependent upon the type and thermal/physical properties of the refrigerant used, and structural/geometrical parameters of refrigerant flow channels. The refrigerant-based PV/T can achieve maximum electrical efficiency of around 10% and thermal efficiency of around 65% [3].

### NEW ADVANCEMENT

The use of optimized working fluid like nanofluid was proposed through a numerical study by Zhao *et al.* [17]. The system consists of a PV module using c-Si solar cell and a thermal unit based on the direct absorption collector (DAC) concept. First the working fluid of the thermal unit absorbs the solar infrared radiation. Then, the remaining visible light is transmitted and converted into electricity by the solar cell. The arrangement prevents the excessive heating of the solar cell. The system works for both non-concentrated and con-

centrated solar radiation. The optical properties of the working fluid were optimized to maximize the transmittance and the absorptance of the thermal unit in the visible and infrared part of the spectrum, respectively [18, 19].

Gangadevi *et al.* [15] investigated the solar PV/T system using nanofluid (nanoparticles suspended fluid) as working fluid. The whole system was a bit complex because heat exchangers were used to transfer heat to water to heat it up for domestic or other usage. The Al<sub>2</sub>O<sub>3</sub>/water nanofluid is used and the nanoparticle size is 50 nm. The nanoparticles are mixed in the base fluid -water. The mixing process includes sonication and magnetic stirring. Figure 30 shows the image of suspended nanoparticles in the water after sonication in that the nanoparticles are distributed more evenly. The experimental setup consisted of three storage tanks. The first storage tank is used for storing the nanofluid and the other two are used to store city water and hot water respectively.

**Table 3: Summary of Performance of Solar Collector Using Nanofluids.**

Author	Type of collector	Type of nanofluids	Particle size (nm)	Volume fraction (%)	Results
Chougule <i>et al.</i> [20]	Flat-plate	CNT/water	D = 10–12. L = 0.1–10 μ	0.15 wt %	At 50° tilt angle both working fluids gave better performance as compared to the standard normal angle in both conditions. Average collector efficiencies for water and nanoworking fluid are increased 12 and 11% at 31.50° tilt angle, while 7 and 4% respectively at 50° tilt angle using the tracking system
Tiwari <i>et al.</i> [21]	Flat-plate	Al <sub>2</sub> O <sub>3</sub> /water	-	0.5–2 wt %	Using the 1.5% particle volume fraction of Al <sub>2</sub> O <sub>3</sub> nanofluid increases the thermal efficiency as well as kg CO <sub>2</sub> /kWh saving in a hybrid mode of solar collector in comparison with water as the working fluid by 31.64%
Yousefi <i>et al.</i> [22]	Flat-plate	Al <sub>2</sub> O <sub>3</sub> /water	15 nm	0.2, 0.4	For 0.2 wt% the efficiency increases up to 28.3%. The surfactant causes an enhancement in heat transfer efficiency is 15.63%
Yousefi <i>et al.</i> [23]	Flat-plate	MWCNT/water	10–30 nm	0.2, 0.4	The 0.2 wt% MWCNT nanofluids without surfactant decrease the efficiency and to surfactant increase its collector efficiency increases with increase in the volume fraction compared with water.
Yousefi <i>et al.</i> [24]	Flat-plate	MWCNT/water	10–30 nm	0.2 wt%	The more differences between the pH of nanofluids and pH of isoelectric point cause the more enhancements in the effi-

					ciency of the collector
Tyagi et al. [25]	Direct absorption	Al <sub>2</sub> O <sub>3</sub> /water	Less than 20 nm	0.1–5 wt%	The efficiency of a DAC using nanofluid is up to 10% higher than that of a flat-plate collector. Efficiency increases for nanofluids up to 2 wt%
Otanicar and Golden [26]	Direct absorption	Graphite/water, EG	-	0.1 wt %	Using nanofluids solar collector leads to approximately 3% higher levels of pollution offsets than a conventional solar collector
Otanicar et al. [27]	Direct absorption	CNT, graphite, and silver/water	D = 6–20 and L = 1–5 × 10 <sup>3</sup> nm, D = 30, D = 20–40 nm	0–1 wt%	For 30 nm graphite, a maximum improvement, over a conventional flat surface absorber, of 3% With 20 nm silver an efficiency improvement of 5%. An enhancement in the efficiency compared with pure water until 0.5 with.
Saidur et al. [28]	Direct absorption	Al <sub>2</sub> O <sub>3</sub> /water	1, 5, 10, 20	2 wt%	1.0% showing satisfactory improvement to solar absorption, aluminum nanofluids was a good solution for direct solar collector compared to others
He et al. [29]	Direct absorption	CuO/water	20, 50 nm	0.01, 0.02, 0.04, 0.1, 0.2 wt%	The transmittance of Cu–H <sub>2</sub> O nanofluids was much less than water, and decreases with increasing nanoparticle size, mass fraction and optical depth. The highest temperature of Cu–H <sub>2</sub> O nanofluids (0.1 wt %) can increase up to 25.3% compared with water.
Taylor et al. [30]	Direct absorption	Graphite, Al <sub>2</sub> O <sub>3</sub> , Cu/therminol VP-1	20 nm	0.1 wt%	Enhancement in efficiency of up to 10% as compared to surface-based collectors
Liu et al. [31]	Evacuated tubular	CuO/water	50 nm	1.2 wt%	The solar collector integrated with open thermosyphon has a much better collecting performance Increase the collecting efficiency, max and mean value increase to 6.6 and 12.4%, respectively
Risi et al. [32]	Transparent parabolic trough	(0.25% CuO, 0.05% Ni)/ water	-	0.01–0.3	The optimization procedure find a maximum solar to thermal efficiency equal to 62.5%, for a nanofluids outlet temperature of 650 °C and a nanoparticles volume concentration of 0.3%
Lenert et al. [33]	Concentrated parabolic	C–Co/VP-1	10–100 nm	-	Efficiency increases with increasing nanofluids height and solar flux. The optimum optical thickness for a non-selective receiver is 1.7.
Khullar et al. [34]	Concentrated parabolic	Al <sub>2</sub> O <sub>3</sub> /VP-1	5 nm	-	The NCPSC has the potential to harness solar radiant energy and higher efficiency about 5–10% as compared to the conventional parabolic solar collector.
Nasrin et al. [35]	Glass cover plate and sinusoidal absorber	Al <sub>2</sub> O <sub>3</sub> /water	-	5 wt%	The Al <sub>2</sub> O <sub>3</sub> nanoparticles with the highest Pr were established to be most effective in enhancing performance of heat transfer rate than base fluid

Lu <i>et al.</i> [36]	Evacuated tubular	CuO/water	50 nm	0.8–1.5 wt%	Enhance the thermal performance of the evaporator. and evaporating HTC increase by about 30% compared with those of deionized water The HTC in the evaporation section and the 1.2 wt% corresponds to the optimal heat transfer enhancement
-----------------------	-------------------	-----------	-------	-------------	------------------------------------------------------------------------------------------------------------------------------------------------------------------------------------------------------------------------------------------------

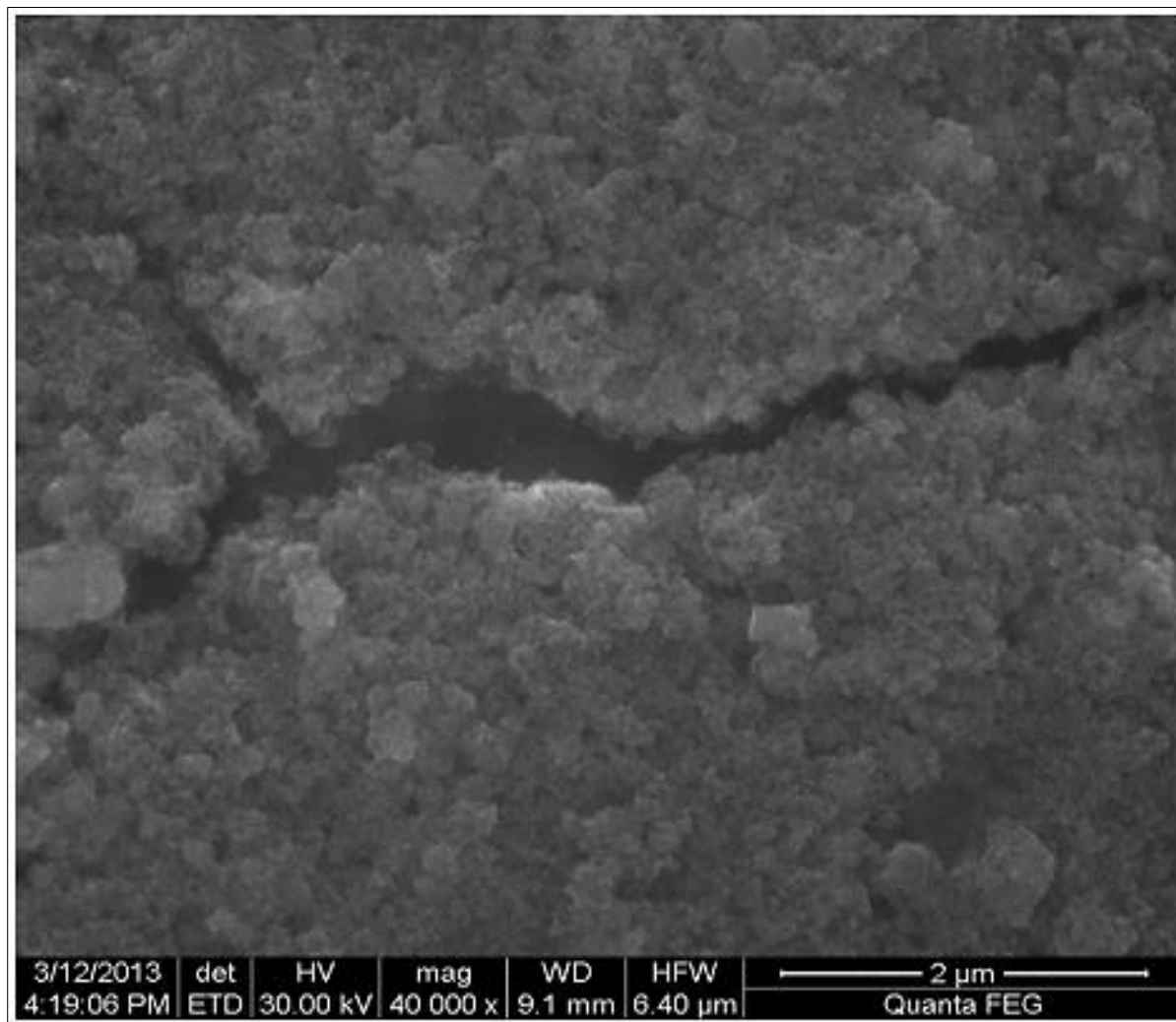


**Fig. 30:** SEM Image of Al<sub>2</sub>O<sub>3</sub>/Water (0.5 Volume %) [15].

A pump is used to pump nanofluid into the solar collector, the output of the solar collector is attached to the heat exchanges that exchange the heat from hot nanofluid to cold water then the cold water becomes hot water by circulation the nanofluid to the thermal collector. In this setup two types of sensors are used to monitor the water temperature and water level. When water gets heated sufficiently it is released for household purposes. Further the sensor also checks the temperature of the nanofluid and releases water into the solar col-

lector so as to cool down the fluid. Further using nanofluid having excellent heat transfer characteristics in the thermal collector, the electrical efficiency of the PV panel as well as the thermal efficiency of the solar collector would increase compared to conventional working fluid.

### CONCLUSIONS

The researches established on PV/T technology were very substantial and mainly focused on (1) revealing the nature of the energy trans-

fer and conversation occurring in the PV/T modules and modules-based system; (2) identifying the favorite the system type; (3) optimizing the structural/geometrical parameters of the system configuration and suggest the appropriate operational conditions; (4) building the link between the theoretical analyses and practical application; and (5) analyzing the economic, environmental benefits of the PV/T systems and evaluating their feasibility for long term operation. All these efforts aimed to create as much energy efficient PV/T system as possible at the least possible cost and simplest structure. However, based on the overview of research conducted to date, it is apparent that there is still a large amount of work that needs to be undertaken in terms of design aspects before PV/T systems can be successfully implemented and integrated into domestic and commercial applications. With an optimum design, PV/T systems can supply buildings with 100% renewable electricity and heat in a more cost-effective manner than separate PV and solar thermal systems and thus contribute to the long-term international targets on implementation of renewable energy in the built environment.

There is possibility to create dual type PV/T system where glass cover over the PV panel can be put on or removed according to the requirement of the season- summer and winter where the electrical and thermal performance can be set respectively.

## NOMENCLATURES

$I_{SC}$	Short circuit current
$V_{OC}$	Open circuit voltage
$h$	Heat transfer co-efficient
$k$	Thermal conductivity
$Nu$	Nusselt's number
$D$	Diameter
$W_p$	Peak Watt
kWh	KiloWatt hour (1 unit)
$Al_2O_3$	Aluminum oxide
CuO	Copper oxide
$CO_2$	Carbon dioxide

## ABBREVIATIONS

AM	Air mass
PV	Photovoltaic

STC	Standard testing condition
PV/T	Photovoltaic and thermal
PVC	Polyvinyl chloride
CPC	Circular parabolic collector
BIPV	Building integrated photovoltaic
BIPV/T	Building integrated photovoltaic and thermal system
G2G	Glass to glass
G2T	Glass to tedlar
CNT	Carbon nanotubes
MWCNT	Multi wall carbon nanotubes
HTC	Heat transfer coefficient

## REFERENCES

1. Kalogirou SA, Tripanagnostopoulos Y. *Energy Conversion and Management*. 2006; 47: 3368–82p.
2. "Effect of Temperature" < [http:// pveducation.org/pvcdrom/solar-cell operation/ effect-of-temperature](http://pveducation.org/pvcdrom/solar-cell-operation/effect-of-temperature) >, Date: 9th January, 2015.
3. Zhanga X, et al. *Renewable and Sustainable Energy Reviews*. 2012; 16: 599–617p.
4. Tiwari GN, Dubey S. *History of PV-integrated Systems*. 2010; 29–73p.
5. Charalambous PG, et al. *Applied Thermal Engineering*. 2007; 27: 275–86p.
6. Dubey S, et al. *Applied Energy*. 2009; 86: 2421–28p.
7. Othman MY, et al. *Renewable Energy*. 2013; 49: 171–74p.
8. Kim JH, Kim JT. *Energy Procedia*. 2012; 30: 1016–24p.
9. Dubey S, Tiwari GN. *Solar Energy*. 2009; 83: 1485–98p.
10. Kim JH, Kim JT. *Energy Procedia*. 2012; 30: 144–51p.
11. Jaiganesh K, Duraiswamy K. *International Journal of Engineering and Technology*. 2013; 5(4). ISSN: 0975–4024.
12. Chow TT, et al. *Applied Energy*. 2009; 86: 689–96p.
13. Abu Baker MN, et al. *Renewable Energy*. 2014; 67: 153–64p.
14. Fang G, et al. *Energy and Buildings*. 2014; 78: 215–21p.
15. Gangadevi R, et al. *International Journal of Engineering Research and Technology*. 2013; 6(6): 747–52p.
16. Tripanagnostopoulos Y. *Solar Energy*. 2007; 81: 1117–31p.



17. Zhao J, et al. *Energy Conversion and Management*. 2011; 52(2): 1343–53p.
18. Chow TT, et al. *International Journal of Photoenergy*. 2012; 1–17p.
19. Mishra RK, Tiwari GN. *Solar Energy*. 2013; 90: 161–73p.
20. Chougule SS, et al. In: *Proceedings of IEEE international conference on advances in engineering, science and management (ICAESM)*. 2012; 247–53p.
21. Tiwari AK, et al. *International Journal Emerging Technology Advanced Engineering*. 2013; 3: 221–24p.
22. Yousefi T, et al. *Renewable Energy*. 2012; 39: 293–98p.
23. Yousefi T, et al. *Experimental Thermal Fluid Scientific*. 2012; 39: 207–12p.
24. Yousefi T, et al. *Solar Energy*. 2012; 86: 771–79p.
25. H. Tyagi et al. *Journal of Solar Energy Engineering*. 2009; 131: 1–7p.
26. Otanicar TP, Golden JS. *Environmental Science Technology*. 2009; 43: 6082–87p.
27. Otanicar TP, et al. *Journal of Renewable Sustainable Energy*. 2010; 2: 033–102p.
28. Saidur R, et al. *International Journal of Heat Mass Transfer*. 2012; 55: 5899–5907p.
29. He Q, et al. *Energy Conservation Management*. 2013; 73: 150–57p.
30. Taylor RA, et al. *Journal of Renewable Sustainable Energy*. 2011; 3: 023–104p.
31. Liu Z–H et al. *Energy Conservation Management*. 2013; 73: 135–43p.
32. de Risi A, et al. *Renewable Energy*. 2013; 58: 134–39p.
33. Lenert A, Wang EN. *Solar Energy*. 2012; 86: 253–65p.
34. Khullar V, et al. *Journal of Nanotechnology Engineering Med*. 2013; 3: 1003–12p.
35. Nasrin R, et al. *Process Engineering*. 2013; 56: 54–62p.
36. Lu L, et al. *Solar Energy*. 2011; 85: 379–87p.

**Cite this Article:**

Karan C. Prajapati, Jatin Patel. Recent Developments in Solar Photovoltaics and Thermal Hybrid Technology. *Journal of Alternate Energy Sources and Technologies*. 2015; 6(1): 14–34p.